Investigation of polymer crystallization kinetics with time dependent light attenuation measurements

J. Fritsch*, W. Stille, G. Strobl

Physikalisches Institut, Albert-Ludwigs-Universität, 79104 Freiburg, Germany

*corresponding author

Abstract

Results obtained for samples of syndiotactic polypropylene and poly(ethylene-*co*-octene) demonstrate the usefulness of light attenuation measurements in investigations of polymer crystallization. The earlier stages with separated growing spherulites fall in the range of Rayleigh-Debye-Gans scattering. Known relationships describing the dependence of the linear attenuation coefficient on the radius and the index of refraction of a spherulite can be applied in evaluations. The sensitivity of attenuation measurements is much higher than that of conventional tools.

1 Introduction

Investigations of the kinetics of polymer crystallization are usually carried out with the aid of differential scanning calorimetry, X-ray scattering in the wide and small angle range, dilatometry, time dependent vibrational spectroscopy or light scattering experiments. Although based on different properties and probing different physical values to derive information about a sample's crystallinity, all these methods end up having a similar sensitivity: reliable data can only be obtained for crystallinities already in the range of some percent of the final value. Reaching end sizes in the order of several microns, the earliest growing spherulites which can be detected by these measurements have already sizes of several hundred nanometers. This, however, is far away from the initial stages of spherulite nucleation and growth.

These early stages have recently gained particular importance in the discussion of the basic mechanisms of polymer crystallization. There are several experimental observations that lead to the assumption of a crystal nucleation and growth which includes an intermediate phase, although a commonly accepted view did not yet evolve. Some authors propose a preceding coverage of the whole volume by a mesomorphic phase which develops by a mechanism resembling a spinodal process [1, 2] while others point at indications for a nucleation into a mesomorphic phase [3]. In our group we favour a view which assumes a mesomorphic phase right in front of a growing spherulite [4].

Trying to scrutinize these different proposed paths of crystallization we searched for an experimental tool with a sensitivity superior to that of the conventional methods, hence being able to survey crystallization over a larger dynamic range. During the last years we approached this aim by performing time dependent light attenuation measurements investigating a sample's turbidity during crystallization, using the standard set-up of small angle light scattering measurements [5]. Such transmission measurements have the potential for a sensitivity higher than the light scattering experiments, since

- the decrease in the transmission is due to photons scattered in all directions, whereas the area of the CCD detector is limited, and

- it is irrelevant whether a photon is scattered once or several times.

Indeed, it was found that the detectable range of crystallization could be somewhat extended [6]. However, the sensitivity of the technique was limited by the inexact restriction of the integration area of the employed CCD detector to a circular region which should just catch the primary beam, by a poor signal-to-noise ratio of the integrated counts and by intensity fluctuations of the laser light source. In order to overcome these experimental deficiencies we now developed a novel device which is dedicated to light attenuation measurements. It is based on a comparison of a beam passing through a sample with a reference beam, both being commonly produced by a chopper modulated laser light source, employing lock-in signal detection. As described in this communication the new device yields results with a large increase in sensitivity.

In fact, light attenuation ('turbidity') measurements have already been applied in crystallization studies, but only in a few cases rather long ago [7, 8, 9, 10], being at this time used for qualitative purposes only. By introducing established theoretical relationships for the total cross section for light scattering we have now put the evaluation on a firm basis. In the following we will present our first results which were obtained for crystallizing samples of syndiotactic polypropylene and poly(ethylene-*co*-octene).

2 Theoretical background

The attenuation of the light intensity after a passage through a plate-like sample with thickness D is described by the Lambert-Beer law

$$\frac{I}{I_0} = \exp(-\Lambda D) \quad , \tag{1}$$

where I_0 denotes the flux of the light beam at the sample front and I represents the flux remaining after the beam has passed through the sample. The parameter Λ is the linear attenuation coefficient which can in general be due to both scattering and absorption of light. For the polymers under study the contribution arising from an absorption is negligible for the applied wavelength of $\lambda = 635$ nm.

Experiments were carried out for samples cooled down from temperatures above the equilibrium melting point to a preset crystallization temperature. Changes of the attenuation coefficient during the crystallization process are due to a growth of spherulites or hedrites, both representing centers of light scattering incidents. Their contribution to the linear attenuation coefficient Λ can be expressed by equations. As long as the scattering objects are diluted in the matrix, which is always the case during the initial stages of the crystallization process, Λ is given by

$$\Lambda = \rho\sigma^2 \quad , \tag{2}$$

where ρ describes the number density of objects and σ^2 represents the total scattering cross section. σ^2 is usually written as

$$\sigma^2 = \pi R^2 Q \quad . \tag{3}$$

Here, R denotes the radius of the scattering object. Q is called 'scattering efficiency factor'. This scattering efficiency factor is dependent on the size of the scatterer as well as on the refractive indices of scatterer, n_{s}, and surrounding material, n_{m}. Together they determine the refractive index ratio

$$m = \frac{n_{\mathrm{s}}}{n_{\mathrm{m}}} \quad . \tag{4}$$

A commonly used variable in describing scattering phenonema is the parameter α, defined as

$$\alpha = \frac{2\pi n_{\mathrm{m}} R}{\lambda} \quad , \tag{5}$$

which is proportional to the radius R. Explicit expressions for Q exist only for spherical scatterers isolated in a matrix, and they are given in the literature[11]. One distinguishes between three

different ranges for α, and they are addressed as

- 'Rayleigh scattering', for $\alpha < 1$,

- 'Rayleigh-Debye-Gans scattering' (RDG), for $1 < \alpha < (m-1)^{-1}$,

- 'Mie scattering', for $\alpha > (m-1)^{-1}$.

As spherulite nucleation starts in the range of some nanometers and growth then proceeds up to several micrometers, corresponding to $0.015 < \alpha < 150$, one is here within the Rayleigh and the Rayleigh-Debye-Gans regime. The scattering efficiency factor in the Rayleigh-Debye-Gans approximation, Q_{RDG}, is given by

$$\begin{aligned} Q_{\mathrm{RDG}} &= (m-1)^2\Big[\frac{5}{2} + 2\alpha^2 - \frac{\sin(4\alpha)}{4\alpha} - \frac{7}{16\alpha^2}(1-\cos(4\alpha)) \\ &\quad +(\frac{1}{2\alpha^2} - 2)(0.577 + \ln(4\alpha) + \mathrm{Ci}(4\alpha))\Big] , \end{aligned} \tag{6}$$

with

$$\mathrm{Ci}(x) = -\int_{\mathrm{x}}^{\infty} \frac{\cos x'}{x'}\mathrm{d}x' \quad . \tag{7}$$

Equation (6) includes the Rayleigh regime as a limiting case for $\alpha < 1$. An analysis of Eq.(6) reveals for $\alpha > 1$ an approximate proportionality of the scattering efficiency factor Q_{RDG} to the squared radius R^2, thus resulting in a dependence of the total scattering cross section σ^2 on the objects radius R given by:

$$\sigma^2_{\mathrm{RDG}} \sim (m-1)^2 R^4 \, . \tag{8}$$

Including calculations for the adjacent Rayleigh and Mie ranges, one can display the radius dependence of σ^2 over a broader interval of radii, as done in [5] for the example of a low density polyethylene. Figure 1 reproduces the results of this calculation. Noticeable are the rather sharp transitions between the three ranges with their different radius dependencies, here located at about 50 nm and 20 μm.

As pointed out above, the introduced equations only hold as long as the scattering objects are isolated in the matrix. Application of the equations ends, when the objects start touching each

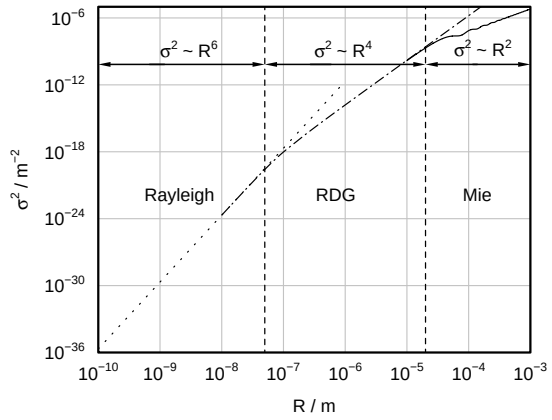

Figure 1: Scattering cross section σ^2 of spheres with radius R for $m = 1.0034$. Calculations were carried out using: Rayleigh approximation (dotted line), RDG approximation (dash-dotted line) and Mie approximation (solid line).

other. In fact, the attenuation coefficient passes over a maximum for an about 50 percent coverage of the sample with scattering objects and subsequently decreases again until homogeneity is reached when the sample is fully occupied by objects. Light attenuation then still exists due to the varying birefringence within the spherulites. It is caused by variations in the orientation of the optical indicatrix, whose direction in the spherulites changes with the orientation of the crystallized chains. The at first dominant scattering caused by the density difference between the melt and the spherulites has disappeared at the end. This time dependence during the later stages has been discussed in qualitative terms already long ago by Hawkins and Richards [7]. Even though there exists a basic understanding, we made no attempt to quantitatively evaluate the kinetics within this part of the measured curves; our focus was on the initial stages of polymer crystallization only.

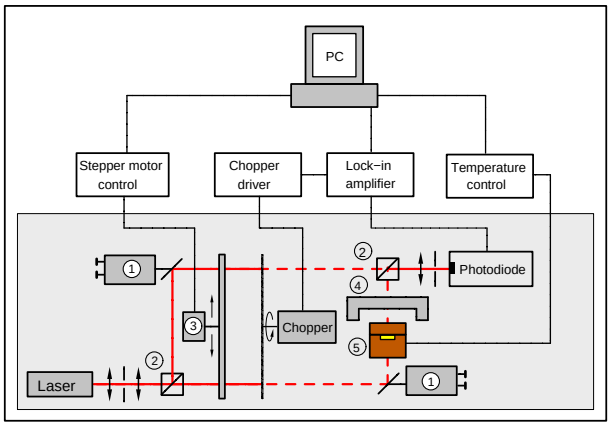

Figure 2: Experimental set-up for light attenuation measurements. 1: adjustable mirrors, 2: beam splitters, 3: selective beam attenuator, 4: heat shield, 5: sample oven.

3 Experimental

We carried out the transmission measurements using a chopper modulated two-beam set-up together with lock-in signal detection. The experimental set-up is displayed in Fig. 2. The utilized light source is an intensity stabilized semiconductor laser module manufactured by Global Lasertech, which operated at a wavelength of $\lambda = 635$ nm with a power of 5 mW. It comprises a built-in monitor photo diode and a processor controlled feed-back circuit to suppress intensity fluctuations. After passage through a spacial filter the laser beam is split up into two beams of equal intensity, one passing through the sample - in the following addressed as the sample beam - while the other is led around the sample, serving as a reference - therefore being addressed as the reference beam. Both beams are now directed through a selective beam attenuator - providing at the beginning of the crystallization experiment a precise intensity match of sample and reference beam by attenuating either one or the other - onto a light chopper which alternately transmits only one beam at a time. After passage through the oven containing the sample, the periodically interrupted sample beam is merged again with the opposite phase modulated refer-

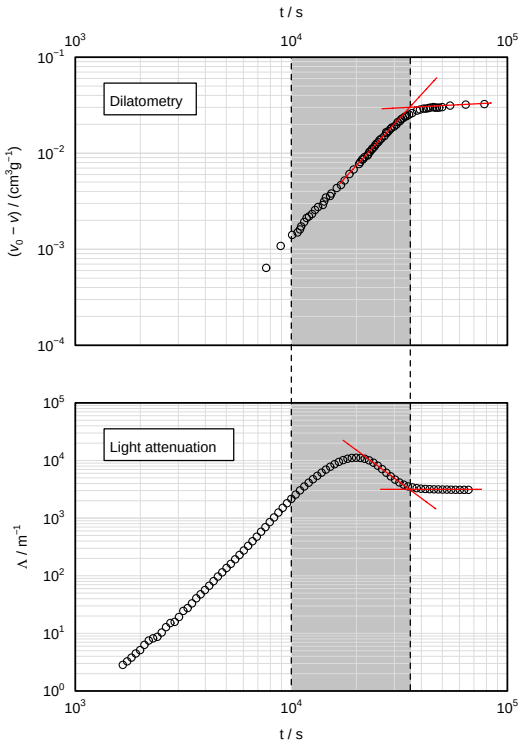

Figure 3: Comparison of two crystallization isotherms of a s-PP sample, obtained by a dilatometric and an attenuation measurement for a crystallization temperature of 115 °C.

ence beam by a second beam splitter. The conjunct laser beam is now focused on a pin hole and directed onto a photo diode. The described set-up allows the application of a lock-in amplifier for phase-sensitive detection at the chopper frequency, as done in our experiment using a Stanford Research Systems model SR830. The output signal of the lock-in amplifier is proportional to the intensity difference between sample and reference beam. Data of the time dependent measurements are stored in a PC for further evaluation. Detailed information concerning data acquisition and analysis is included in [12].

The investigated samples were kept between two glass slides and had thicknesses ranging from

25 μm up to 500 μm, chosen according to their final turbidity in the crystalline state. In order to achieve high cooling rates, thus being able to measure also low temperature isotherms with short crystallization times, the sample was heated in an external hot stage and then transferred into the sample oven preset at the crystallization temperature, reducing the cooling process down to less than 30 seconds.

The polymers under study were a commercial syndiotactic polypropylene with 83 % syndiotactic pentades, sPP, produced by Fina Co., Brussels, and a poly(ethylene-*co*-octene) of the metallocene catalyst type with an octene weight content of 14 %, P(EcO14), supplied by Dow Chemicals Europe.

4 Results

A crystallization isotherm of sPP measured with the set-up is displayed in Fig. 3 and compared to an isotherm obtained by a dilatometric measurement. The improvement of the sensitivity resulting in an extension of the observable period of crystallization by nearly one order of magnitude, is clearly visible.

Figure 4 displays a series of time dependent transmission measurements expressed in terms of Λ, carried out for sPP at different crystallization temperatures. They all exhibit the expected characteristic form: Starting with a constant slope, they reach a maximum for an about 50 % volume coverage of the polymer sample by scattering objects, and subsequently decrease as the scatterers grow further until they fill the whole sample. As already mentioned, the non-vanishing final value is caused by the varying birefringence of the partially crystalline scattering objects. If the crystallization temperature increases, the measured isotherms are shifted towards longer times - approximately one decade every 15 K. In the range of higher crystallization temperatures one only observes a parallel shift of the isotherms, all having an initial slope of about 5, corresponding to a power law $\Lambda \sim t^5$, as indicated by the dashed line. This slope is

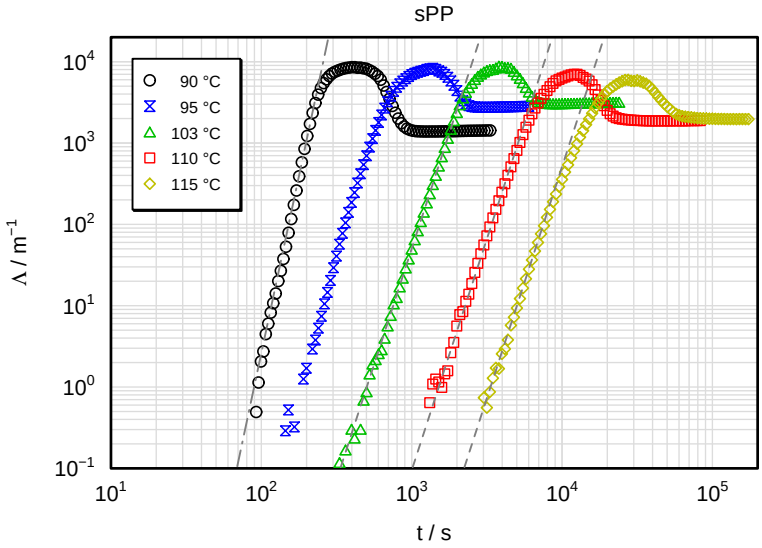

Figure 4: Crystallization isotherms of a sPP sample in terms of Λ. The sample thickness is 500 μm. The dashed line indicates an initial power law $\Lambda \sim t^5$, while the dash-dotted line is representative for $\Lambda \sim t^8$.

constant within each isotherm through three orders of magnitude of the attenuation coefficient Λ, before reaching the maximum related with a 50 % coverage. Going down to lower crystallization temperatures an increase in the slope of the isotherms is observed, reaching a value of 8, i.e., indicating $\Lambda \sim t^8$, for a crystallization temperature of 90 °C (dash-dotted line).

Figure 5 displays the isotherms measured for a poly(ethylene-*co*-octene) sample with a thickness of 500 μm. For each isotherm the slope remains constant through nearly 4 orders of magnitude, until the maximum of Λ is reached. At the highest temperatures slopes are rather low and then they increase when the crystallization temperature is decreased, from values of 2 for the highest (94 °C) up to 6 for the lowest used crystallization temperature (84 °C). Another observation to be noticed in Fig. 5 is the drop of the maximum value of Λ for increasing crystallization temperatures.

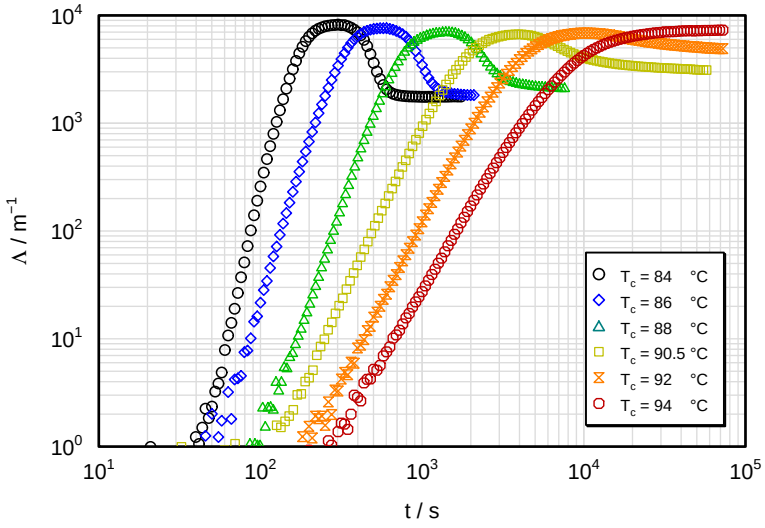

Figure 5: Crystallization isotherms of a sample of P(EcO14). The sample thickness is 500 μm.

5 Discussion

The dilatometric crystallization isotherm of sPP in Fig. 3 was taken from a series of measurements reported previously [13]. The slope in the $\log - \log$ plot indicated for the initial stages of the crystallization process a decrease of the specific volume proportional to t^3 for all crystallization temperatures. Such a behavior is expected if the growing objects - hedrites or spherulites - increase in size with a constant growth rate, i.e., for

$$R \sim t \quad . \tag{9}$$

One then expects for the time dependence of the linear attenuation coefficient Λ the power law

$$\Lambda \sim R^4 \sim t^4 \quad . \tag{10}$$

This is indeed found for Λ within the time- and crystallization temperature range of the dilatometric measurements. However, the initial slope, i.e., the one observed in the preceding time range which could not be accessed by dilatometry, is higher, amounting to a value of about 5. Here, an additional contribution to the scattering efficiency exists and it could arise from a

change in the inner crystallinity of the scatterers. This would lead to a change in the refractive index ratio m and hence to a change of the attenuation coefficient according to the relationship $\Lambda \sim (m-1)^2$. With Eq.(4), and taking into account that

$$n_{\mathrm{s}} = (1-\phi_{\mathrm{c,i}})n_{\mathrm{m}} + \phi_{\mathrm{c,i}} n_{\mathrm{c}} \tag{11}$$

with n_{c} representing the refractive index of crystallites, one obtains

$$\Lambda \sim \phi_{\mathrm{c,i}}^2 \quad , \tag{12}$$

where $\phi_{\mathrm{c,i}}$ represents the inner crystallinity of the scattering objects. The measured slope of 5, obtained for the sPP sample when crystallized at high temperatures, can therefore be understood as resulting from two factors, namely a growth of a spherulite which is accompanied by a simultaneous increase of the inner crystallinity.

Not yet understood is the mechanism that leads to the initial power law $\Lambda \sim t^8$ observed for the lowest crystallization temperature. There are no results of other measurements which could be consulted, as all known experiments do not enter this domain of short crystallization times at low crystallization temperatures.

The investigated poly(ethylene-co-octene) sample exhibits crystallization isotherms with $\log - \log$ plot slopes varying from approximately 2 to 6 - again the slope is increasing when the crystallization temperature decreases. According to Eq.(12) isotherms with a slope of two, as they are measured for the highest crystallization temperature, have to be interpreted as resulting from a first order in-filling process of crystallites into objects of virtually constant size. This increase of the inner crystallinity can be observed over two orders of magnitude, corresponding to four orders of magnitude in Λ. On the other hand, the creation of the objects that become filled by the crystallites is not detected. The same kinetics of in-filling had already been observed in investigations of P(EcO14) with a polarizing optical microscope [14]. Here, a diffuse 'precursor' structure with length scales in the micrometer range showed up already at

the beginning of the structural observations and then increased in contrast. The observation also indicated an increase in the inner crystallinity of given objects without changes in their geometry. The fact that the creation of the precursor structure is still not detected when using the much more sensitive attenuation measurements means that the mass density difference against the melt of these objects in the initial, empty state, $\Delta\rho_{\mathrm{in}}$, is extremely low indeed. As we follow the filling process over two orders of magnitude, $\Delta\rho_{\mathrm{in}}$ must be below 10^{-4} g cm^{-3} (the completely filled objects show a mass density difference $\Delta\rho \approx 10^{-2}$ g cm^{-3} corresponding to an inner crystallinity of about 10%). When the objects are filled they show the birefringence pattern of spherulites. Thinking about the nature of the objects in the initial state, one could speculate that they are built up by a skeleton of a few dominant crystalline lamellae which grew rapidly in advance, prior to the large majority of lamellar crystallites.

Acknowledgements

We highly appreciate the advice which we obtained from Georg Maret (University Konstanz). Funding of this work by the Deutsche Forschungsgemeinschaft is gratefully acknowledged. Thanks are also due to the 'Fonds der Chemischen Industrie' for financial support.

References

[1] Imai M, Kaji K, Kanaya T, Sakai Y (1995) Phys Rev B 52:12696

[2] Olmsted P, Poon W, McLeish T, Terrill T, Ryan A (1998) Phys Rev Lett 81:373

[3] Kraak H, Deutsch M, Sirota E (2000) Macromolecules 33:6174

[4] Strobl G (2000) Eur Phys J E 3:165

[5] Kawai T, Strobl G (2004) Macromolecules 37:2249

[6] B Heck TK, Strobl G (2005) Polymer submitted

[7] Hawkins S, Richards R (1949) J Polym Sci 4:515

[8] Keane J, Stein R (1956) J Polym Sci 20:327

[9] Levy B (1961) J Appl Polym Sci 5:408

[10] Mahen K, James W, Bosch W (1965) J Appl Polym Sci 9:3605

[11] Kerker M (1969) The Scattering of Light. Academic Press, p. 418

[12] Fritsch J (2005) Diplomarbeit. Physikalisches Institut, Universität Freiburg

[13] Heck B, Strobl G (2004) Colloid Polym Sci 282:511

[14] Häfele A, Heck B, Kawai T, Kohn P, Strobl G (2005) Eur Phys J E 16:207